Journal of Innovative Optical Health Sciences
Vol. 9, No. 4 (2016) 1642002 (11 pages)

DOI: 10.1142/S1793545816420025

Fluorescent and quantitative mitochondrial redox imaging of tumor targeted by Octa-RGD probe

Shuang Sha[*,†,§], Fei Yang[*,†,§], Anle Wang[*,†], Honglin Jin[*,†], Zhihong Zhang[*,†] and Qiaoya Lin[*,†,‡]

[*]*Britton Chance Center for Biomedical Photonics*
Wuhan National Laboratory for Optoelectronics–Huazhong University of Science and Technology
Wuhan 430074, P. R. China

[†]*MoE Key Laboratory for Biomedical Photonics*
Department of Biomedical Engineering
Huazhong University of Science and Technology
Wuhan 430074, P. R. China
[‡]*linqiaoya@hust.edu.cn*

Received 24 November 2015
Accepted 17 March 2016
Published 26 April 2016

Integrins, over-expressed in a broad range of cancer diseases, are widely utilized as a tumor biomarker. Metabolism investigation also plays important roles in tumor theranostics. Developing simple integrin-targetting probe and monitoring tumor metabolism will give opportunities to find ways for cancer treatment, however, the investigation of tumor metabolism with integrin receptor based probes has been rarely reported so far. Here, we developed an octavalent fluorescent probe Octa-RGD by convenient genetic method, based on one tetrameric far-red fluorescent protein (fRFP) linked with RGD peptides. We validated its intergin targeting by confocal imaging *in vitro*. Then we screened a variety of tumor cells, and differentiated their binding affinity based on the fluorescence of the probe via flow cytometry. Among these cells, CNE-2 cells had the highest uptake of the probe, while B16 cells had the lowest, corresponding with their intergin expression levels. Next, the fluorescent and metabolic imaging was performed in HT1080 (intergin postive) tumor, where nicotinamide adenine dinucleotide hydrogen (NADH), flavoprotein (Fp) and fRFP fluorescent signals were collected. The tumor from mice intravenously injected with Octa-RGD probe displayed obviously higher NADH redox ratio NADH/(Fp+NADH) and fRFP signal, than those with fRFP protein. It suggested that integrin targeting may have influence on the target cell metabolism, and further demonstrated Octa-RGD probe facilitated its uptake in the targeted tumor *in vivo*. This paper developed a useful probe, which

‡Corresponding author.
§These authors contributed equally to this study.

can bind integrins specifically and efficiently in tumor cells, and together with tumor metabolic information, it may provide new insight for RGD targeting-based cancer therapeutics.

Keywords: Integrin; redox metabolism; fRFP; NADH; Fp.

1. Introduction

Integrins, one type of the Cell Adhesion Molecules (CAMs), play important roles in cell adhesion, migration, proliferation and apoptosis,[1] and also have important impacts on cancer diseases.[2] Integrins are heterodimeric transmembrane glycoproteins which consists of two subunits α and β,[3] were over-expressed in a variety of tumors, such as lung cancer,[4] breast cancer,[5] head neck squamous cell carcinoma[6] and pancreatic ductal adenocarcinoma[5] but seldom expressed in normal tissues.[5,7] Therefore, it can be an ideal and useful tumor biomarker to target. Labeling integrin antagonists could provide important diagnostic tools for assessing the efficacy of anti-angiogenic or anti-tumor therapies. Many types of integrin have been utilized as cancer therapeutic target, such as $\alpha_v\beta_3$,[8] $\alpha_v\beta_6$ integrins and so on.[9,10]

Recently, many types of probes[11] have been developed and used as radiotracers to target variable integrin receptors on tumor cells surface for molecular imaging, such as PET probe [18^F]FBA-A20FMDV2,[12] micro PET probe ^{64}Cu-DOTA peptide,[13] MRI nanoparticles ^{3}H-LCP-MFM[14] and fluorescent nanoparticles.[15] However, these chemical probes are complicated to obtain, low yield for large-scale preparation, or not metabolized easily in body organs. The genetic engineering has been occurring as a simple method, which has many advantages over chemical synthesis, such as easy purification and good biocompatibility.[16] In the meantime, far-red fluorescent protein (fRFP) with low toxicity has been widely used for *in vivo* optical imaging.[17,18] Thus, we developed a new probe named Octa-RGD, based on a fRFP via biological synthesis with integrin receptor targeting,[19] which can provide a simple and safe method for optical targeted imaging in tumors.

The distribution and degradation of the nano-sized-probes are correlated with tumor microenvironment and metabolism states as literature reported.[20] Tumor metabolism investigation is important and beneficial for understanding cancer cell malignant growth and potential drug resistance, and can give opportunities to find ways for cancer therapeutics.[21,22] Many methods have been developed to investigate the tumor metabolism, such as tumor glycolysis[23] and oxidation measurement by MRI,[24] PET and PET/CT,[25] but these methods are indirect and need exogenous chemical probes to exhibit metabolism states. Chance *et al.* developed a redox scanning method based on a standard metabolic redox pair nicotinamide adenine dinucleotide hydrogen (NADH) and flavoprotein (Fp), which are endogenous autofluorescent coenzymes of mitochondrial respiration chain. Their fluorescence intensities can noninvasively indicate tumor tissue metabolic states and their inner heterogeneous distributions. The metabolic states of tissue *ex vivo* in the liquid nitrogen can be blocked and maintained the same metabolic state *in vivo*.[26] Under this condition, the fluorescence intensities of tissue NADH and Fp is almost 10 times more than those at normal temperature. This redox scanning has been a classic method to monitor the tumor metabolism.[27,28] Nowadays, it has been rarely reported on tumor metabolic imaging with integrin receptor based probes so far. Therefore, observation of these target probes related metabolism states in tumors is attractive and urgent.

In this paper, we developed a probe named Octa-RGD, which can specifically target to integrin receptor of tumor cells both *in vitro* and *in vivo*, and simultaneously be utilized as fluorescent tag. The probe was applied to screen variable tumor cells (HT1080 cells, B16 cells, CNE-2 cells, MDA-MB cells, MCF-7 cells), and we observed that CNE-2 cells, MDA-MB cells and HT1080 cells had higher affinity than B16 cells and MCF-7 cells, corresponding with their different intergin expression levels. Moreover, we investigated the mitochondrial redox state of human fibrocarcinoma-HT1080 tumor targeted by Octa-RGD probe. The tumors from mice injected with Octa-RGD probe displayed obviously higher NADH redox ratio, and significantly higher fRFP signal, than those with fRFP protein. From these results, we can conclude that the Octa-RGD probe has ability to target different

tumor cells specifically both *in vitro* and *in vivo*. This study introduced a new probe to detect cell integrin expression conveniently, and gave some valuable information about the tumor metabolism with integrin receptor based probe distribution.

2. Materials and Methods

2.1. *Construction of Octa-RGD plasmid*

To construct the plasmid Octa-RGD, primers in Table 1 were used. The DNA fragment fRFP-RGD was amplified by PCR first, and then it was used as the template for PCR to obtain the DNA fragment RGD-fRFP-RGD which was collected and digested by the EcoRI and HindIII simultaneously. The plasmid vector pRSET-B was digested under the same condition and ligated with RGD-fRFP-RGD by T4 DNA ligase (Takara, Japan). Since fRFP was a tetramer complex as we had proven previously,[19] the flanking RGD on both ends made RGD-fRFP-RGD an octa-valent probe, termed as Octa-RGD.

2.2. *Protein purification and quantitation*

The bacterium strain BL21 (DE3) was used for protein expression and purification. Octa-RGD and fRFP were purifed and quantitated in the same way. The culture was centrifuged and re-suspended in binding buffer after 12-h induction with 1 mM IPTG. The suspended bacteria were then sonicated for 1 s of every 5 s for a total of 30 min. The lysate was centrifuged at 12,000 rpm for 10 min with the sediments discarded. The supernatant was filtered with 0.45 μm syringe filters and subjected to Ni-NTA His-affinity rasin (Thermo Scientific, USA). After washing the impurities off from the column for several times with washing buffer, the protein of interest was eluted by 500 mM imidazole. The collected protein was dialyzed in PBS over night and run through a 0.22 μm sterilized syringe filter. The concentrations of both purified proteins were quantitated with a Modified Lowry Assay kit (Thermo Scientific, Massachusetts, USA) before use.

Table 1. Octa-RGD plasmid oligonucleotides.

Primer	Sequence (5′-3′)
F-1	CCGGAATTCGTGGGTGAGG ATAGCGTG
F-2	CCCAAGCTTTTAGGTGCGCGCCAC TTTCTGTGCAAGAACCTG
F-3	CTTTCTGTGCAAGAACCTGCAAAT CACCACCGTAAATTCGGAAC
F-4	CCACGTAAATTCGGAACTGCATTG CCACCCACCCATCCGCCGCTG
F-5	GCCACCCGATCCGCCGCT GTGCCCCAGTTTGCTAG
R-1	AAGTTTTAGCGCAAAAAGTGGC ACGAACAGGCGGATCGGGTGG CATGGTGGGTGAGGATAG CGTGCTGATCACCGAG
R-2	CCGGAATTCAACGCGGTGCCTAACCT TCGCGGCGATTTACAAGTTTTAGCG CAAAAAGTGGCACGAACAGGCGG

2.3. *Confocal imaging and flow cytometry*

HT1080, B16, CNE-2, MCF-7 and MDA-MB-435S cells were preserved by our lab. These cells were cultured in RPMI 1640 medium (Gibico, USA) and supplemented with 10% fetal bovine serum (Hyclone, USA) and 100 IU/ml penicillin, 100 μg/ml streptomycin with 37°C 5% CO_2 (Thermo, USA).

For confocal imaging, HT1080 and B16 cells were incubated with the probe Octa-RGD (10 μM) for 2 h, while fRFP as the control. The cells were washed twice with PBS before the 10-minute incubation in 1 μM Hoechst 33258 (Sigma, USA), and transferred to confocal microscopic imaging system (Olympus, Japan) for imaging. The probe was exicted with 543 nm laser and Hoechst with 405 nm. For flow cytometry, each of the aforementioned cell lines were collected and incubated in 10 μM Octa-RGD and fRFP, respectively. After washing twice with PBS, the cells were suspended and subjected to flow cytometry (Guava easay Cyte 8HT, Millipore, German).

2.4. *Characterization of Octa-RGD probe*

The hydrodynamic size distribution of Octa-RGD were measured by light-scattering photon correlation spectroscopy (Zetasizer Nano-ZS90; Malvern Instruments, Malvern, UK) with a 4.0-mW He–Ne laser operating at 633 nm and a detector angle of 90°. For particle size determination, the data were modeled assuming spherical particles undergoing Brownian motion.

The purified Octa-RGD probe and fRFP protein of the same concentration were subjected to SDS-PAGE. 8% polyacrylamide gel was used as the separating gel for SDS-PAGE, and prestained protein ladder (Fermentas, USA) was used as the molecular-weight size marker.

2.5. *Xenograft model in nude mice*

Nude mice (male, 6–8 weeks) were purchased from Silaike company (Shanghai, China). Mice were maintained under SPF conditions, and all experiments were performed according to the animal experiment guidelines of the Animal Experimentation Ethics Committee of HUST. Nude mice were inoculated with 2×10^6 HT1080 cells (in 100 μl PBS) subcutaneously in the left flanks, respectively.

2.6. *The whole body fluorescence imaging*

Two weeks after tumor inoculation, the xenograft-bearing nude mice ($n = 6$) were randomly allocated into two groups. Mice were intravenously injected with the Octa-RGD probe at the concentration of 56 μM in one group, while the other group of mice were i.v. injected with fRFP protein at equal amount of protein. The fluorescence images of the whole body were taken at the time of 30 min, 6 h, 9 h, 12 h post-injection, respectively by using a custom-made whole-body optical imaging system[29] with a deep red filter set (excitation filter: 562/40 nm; emission filter: 655/40 nm). All the images were calibrated with an autofluorescent background filter set (excitation filter: 469/35 nm; emission filter: 655/40 nm) and exposure time of 5 s.

2.7. *Redox scanning*

After the whole body fluorescence imaging, the mice were sacrificed. The tumors were excised, and were frozen in liquid nitrogen quickly. Then the tumor was mounted by refrigerant (ethanol: glycerin: water = 3:6:1). In order to observe tumor metabolism directly and conveniently, we utilized a redox scanner, which is a home-made low temperature imaging system in our lab for monitoring tissue mitochondria NADH and Fp fluorescent signal *ex vivo*. NADH, Fp and fRFP were excited by 365 nm, 455 nm and 590 nm LEDs with exposure time of 1 s, 2 s, 10 s, respectively, and the emission filters we used are 447 ± 30 nm, 546 ± 12.5 nm and 630 ± 12.5 nm. The data was analyzed by the MATLAB 7.0 software as previously described.[27] The fluorescence intensity of the NADH, Fp and fRFP signal was analyzed by the MATLAB 7.0 software as previously described.[30]

3. Results

3.1. *Characterization of Octa-RGD probe*

After synthesizing the Octa-RGD probe by genetic method based on fRFP protein (RGD-fRFP-RGD, abbreviated as Octa-RGD, as the tetrameric fRFP binds eight RGD peptides), we next investigated the property of probe. To determine the hydrodynamic size distribution of probe, the dynamic light scattering (DLS) was used to detect, as shown in Fig. 1(a), the data indicated that the size of Octa-RGD probe is 12 nm ± 1 nm. Sodium dodecyl sulfate polyacrylamide gel electrophoresis (SDS-PAGE) analysis indicated the size difference between Octa-RGD probe and the control tetrameric fRFP

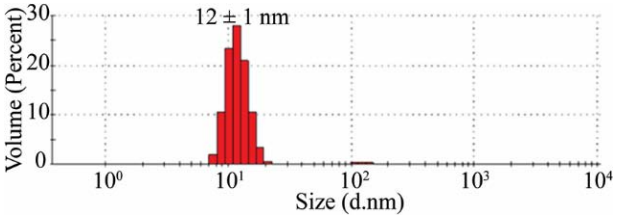

(a)

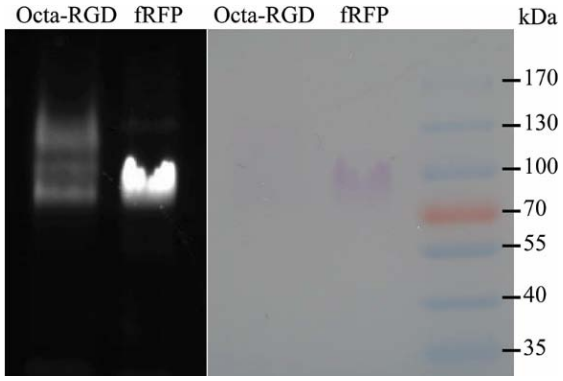

(b)

Fig. 1. Characterization of Octa-RGD probe. (a) The DLS result of Octa-RGD fluorescent probe. (b) The SDS-PAGE analysis of Octa-RGD probe and fRFP protein. The standard protein marker is on the right.

protein, evidenced by their migration difference of gel band in Fig. 1(b). We also had previously shown that those fRFP protein based probes all kept stable after incubated with blood plasma at 37°C for 3 h, and demonstrated that tetramerization enhanced the plasma stability of protein.[19]

3.2. *Validating the targeting of Octa-RGD probe in living cells*

After describing the property and validating the stability of Octa-RGD probe, we next investigated its targeting by using confocal study. Two cancer cell lines were used in this study, HT1080 cells[31] (integrin receptor positive cell line) and B16 cells (minimal integrin receptor expression cell line).[32] As shown in Fig. 2(a), high uptake of Octa-RGD probe was observed in the HT1080 cells visualizing by its strong red fluorescence signal, while minimal signal was observed in B16 cells (Fig. 2(b)). Minimal uptake of fRFP protein was both shown in HT1080 and B16 cells, and no significant difference was found between positive and negative cells in untargeted fRFP group. The data indicated the Octa-RGD probe selectively targeted to integrin receptor positive cells, while fRFP protein did not.

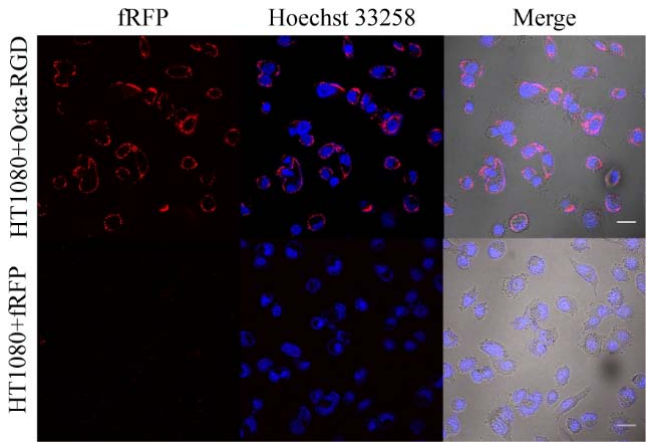

(a)

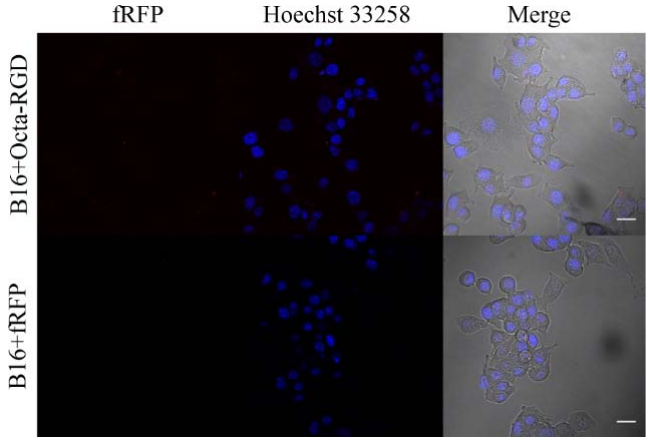

(b)

Fig. 2. Cell uptake of Octa-RGD probe and fRFP protein by confocal imaging. (a) Confocal imaging in HT1080 cells (integrin positive cell line). (b) Confocal imaging in B16 cells (integrin negative cell line). The cells were incubated with 10 μM Octa-RGD or 10 μM fRFP for 2 h as indicated. The cell nucleus was stained with Hoechst 33258. The red signal represented the fluorescence from fRFP, and the blue signal represented the fluorescence from Hoechst 33258. The images were all taken under the same conditions.

3.3. *Screening binding affinity for integrin receptor in different cells by flow cytometry*

After validating the targeting of probe, we next investigated the screening ability of probe on binding affinity for integrin in a variety of tumor cells, including murine melanoma B16 cells, human nasopharyngeal carcinoma CNE-2, human fibrosarcoma HT1080, human melanoma MDA-MB and human breast adenocarcinoma MCF-7 cells. Different cells were incubated with equal amount of Octa-RGD probe and fRFP protein, respectively, then the red fluorescence intensity was analyzed by flow cytometry. As shown in Fig. 3, compared to the fRFP protein group, higher fluorescence intensity ratio of Octa-RGD was found in CNE-2 (19.75), HT1080 (9.6) and MDA-MB cells (10.24), while mininal fluorescence intensity of probe was found in MCF-7 (1.89) and B16 cells (1.54). Comparing the fluorescence intensity of probe in HT1080 cells and B16 cells as mentioned previously, we observed that the fluorescence intensity of probe in HT1080 cells was six folds more than that in B16 cell. This difference was consistent with the confocal study as shown in Fig. 2. It further confirmed the targeting of Octa-RGD probe. The data also indicated that the CNE-2, HT1080 and MDA-MB cells has higher binding affinity for probe, while MCF-7 and B16 cells has minimal binding affinity, the uptake difference of the probe was corresponding with the intergin expression level as previous literature reported.[31–34]

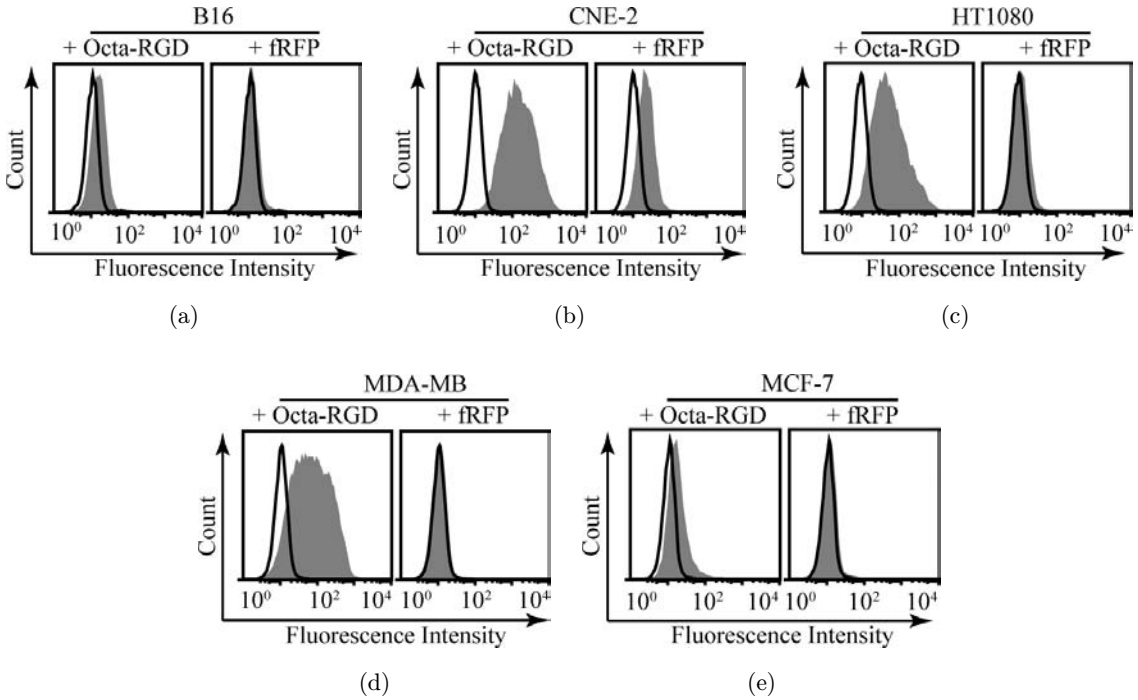

Fig. 3. Flow cytometry plots showing different binding affinity for RGD peptide in different tumor cells. As indicated in the figure, all cells were incubated with the same amount of Octa-RGD probe and fRFP protein, respectively The black curve represents cells alone without incubation, the gray-filled curve represents cells after incubation. The x-axes of the histograms represent the fRFP fluorescence intensity. The y-axes represent the number of pixels in the cells having a specific value of fRFP.

3.4. *The enhanced uptake of Octa-RGD probe in the targeted tumor*

Next, we investigated the *in vivo* targeting of Octa-RGD probe in an integrin receptor positive tumor model (human fibrocarcinoma-HT1080 xenograft model). The equal amount of fRFP protein was also intravenously injected as a control. The whole body fluorescence images were taken at different time points (0.5 h, 6 h, 9 h and 12 h) post-injection. As shown in Fig. 4, the strong red fluorescence signal in tumor region was observed in Octa-RGD group at each time point, while weak signal was found in fRFP protein group. The data indicated that the Octa-RGD probe facilitated its uptake in the targeted tumor *in vivo*.

3.5. *The quantitative mitochondrial redox imaging of tumor targeted by Octa-RGD probe*

Next, to investigate the tumor metabolism state, the Cryo-imager developed previously[30] was used to

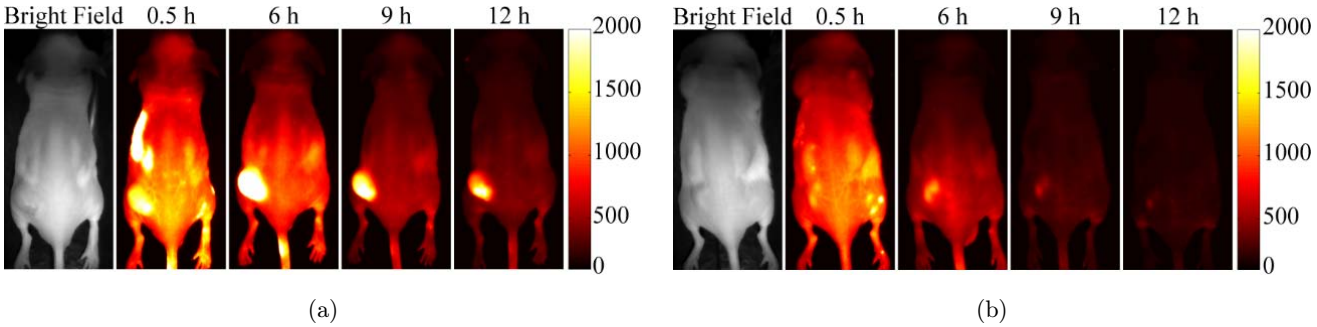

Fig. 4. The whole body images of Octa-RGD fluorescent probe and fRFP fluorescent protein in human fibrosarcoma bearing nude mice at different time point, respectively. (a) Octa-RGD probe group. (b) fRFP protein group. Images were taken under the same conditions at 30 min, 6 h, 9 h, 12 h post-injection, respectively.

detect the NADH and Fp signals of tumors. The supporting Fig. 1 depicted the spectra of NADH, Fp, Octa-RGD and fRFP, respectively, the data demonstrated that there was no crosstalk when we use Cryo-imager system, it can distinguish each signal well. After 12 h post-intravenous injection of probe, the mice were sacrificed and tumors were excised and put into liquid nitrogen immediately to maintain their primary metabolism. Figure 5 showed the metabolic and fluorescent imaging of HT1080 tumor targeted by Octa-RGD probe or control fRFP protein, including Fp, NADH, NADH redox ratio NADH/(Fp+NADH) and fRFP fluorescent signal. As shown in Fig. 5(a), we observed that the region with more Octa-RGD probe accumulated had higher NADH redox ratio in tumor. The correlation analysis was performed to further assess their relationship. However, the R^2 of correlation between NADH and fRFP was less than 0.5, that is, no significant correlation relationship was found (data not shown here).

The tumor with Octa-RGD probe accumulation (Fig. 5(a)) had lower Fp fluorescence intensity, but

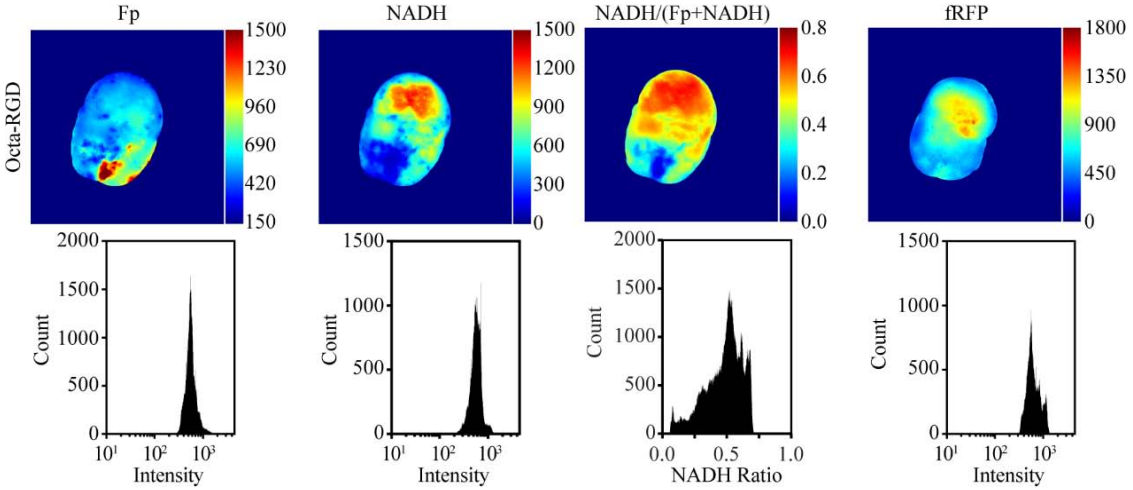

(a)

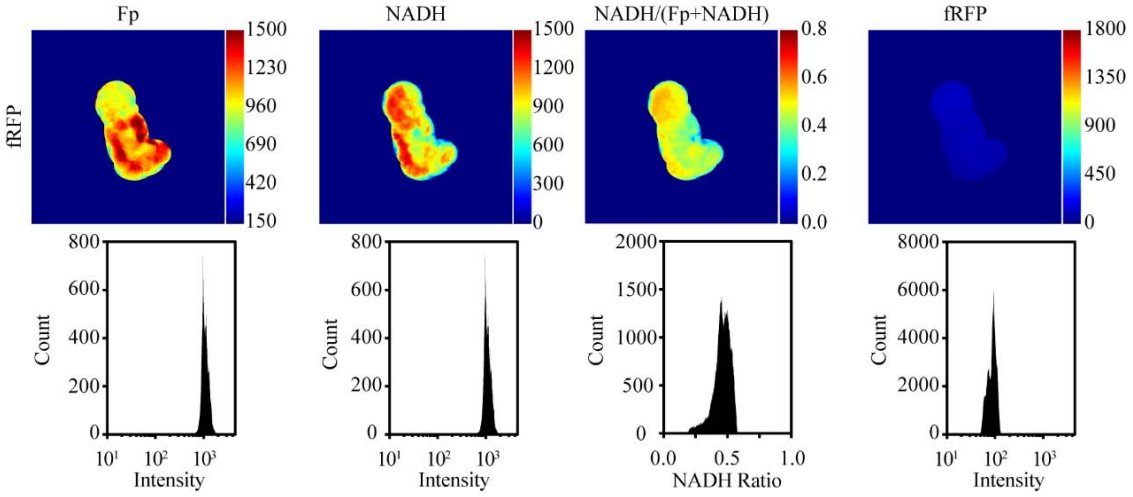

(b)

Fig. 5. The redox and fRFP fluorescence image and corresponding histograms of (a) Octa-RGD probe and (b) fRFP protein in human fibrosarcoma HT1080 tumor regions, respectively. The x-axes of the histograms represent the Fp, NADH, NADH redox ratio NADH/(Fp+NADH) or fRFP fluorescence intensity, respectively. The y-axes represent the number of pixels in the tumor section having a specific value of Fp, NADH, NADH ratio or fRFP. (c) The average NADH redox ratio of tumors with Octa-RGD probe ($n = 5$) or fRFP protein ($n = 10$) uptaken, respectively. (d) The RFP fluorescence intensity of tumors in two groups. Error bars represent SEM. The student's t-test was used to determine significance and p-values less than 0.05 were considered significant ($^*p < 0.05$).

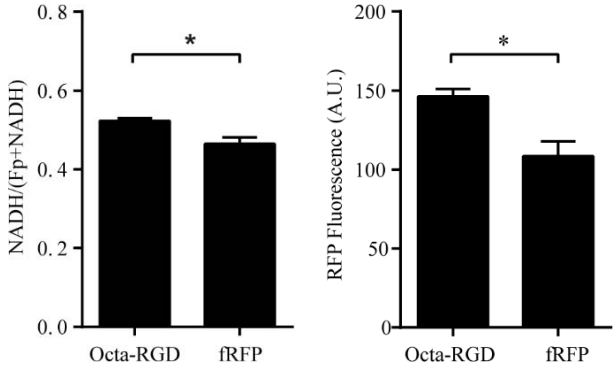

(c) (d)

Fig. 5. (*Continued*)

higher NADH redox ratio NADH/(Fp+NADH) than the tumor with fRFP protein (Fig. 5(b)). The average NADH redox ratio as shown in Fig. 5(c) further confirmed this phenomenon ($p < 0.05$). In addition, the fRFP fluorescent signal in Octa-RGD probe group was found significantly stronger ($p < 0.05$) than the signal in fRFP protein group as shown in Figs. 5(a), 5(b) and 5(d). The data further demonstrated the Octa-RGD probe facilitates its uptake in the targeted HT1080 tumor at tissue section level, it consistent with the whole body fluorescence images shown in Fig. 4. The Fp coenzyme was localized in mitochondria, and it would be reduced after treatment with some oxidative phosphorylation inhibitors as the tissue metabolism shifted as reported.[35] When Octa-RGD probe was delivered to inner tumor via integrin receptor after 12 h post-injection, the decreased Fp signal or increased NADH redox ratio compared to untargeted protein fRFP suggesting that the RGD targeting might change the tumor metabolism.

4. Discussion and Conclusion

Many factors can influence the effectiveness of drug uptake in the solid tumors, such as gene amplification, metabolism, and the limited penetration into tumors.[36] It is important to develop probes to increase the drug uptake ability and know their distribution in the inner tumors, and investigate the relationship between tumor metabolism and their distribution.

Integrin is a high expression receptor in most tumors surface, while nearly no expression in normal tissues. So intergrin targetting-probe can be a useful tool to deliver much more therapeutic drugs to the tumor region.[37] Many chemical synthesis-probes were developed to bind different types of integrin receptors of tumor surface. However, it still lacks a convenient method for developing a probe which can detect and observe integrin receptor expression simultaneously with low toxicity.

In this paper, we developed a new probe named Octa-RGD, based on a tetrameric fRFP, which had ability to target integrin receptor in tumor cell surface with high stability (Fig. 2). It is simple and convenient to synthesize using genetic engineering method. In order to detect the binding affinity of Octa-RGD probe to tumor cells, we incubated probe with five tumor cell lines, respectively. The flow cytometry results (Fig. 3) indicated that different tumor cell lines had varied binding affinity to the probe. CNE-2 cells had the highest affinity than the other cells, while B16 cells had the lowest. This differentiation of binding affinity was corresponding with their different integrin receptor expression levels as reported.[31–34] The data indicated that the Octa-RGD probe could be utilized to evaluate and screen integrin expression in tumor cells. However, further experiments need performing to investigate its specificity and sensitivity thus confirming whether it has the potential to be a simple screening probe in future. Next, the targeting ability of probe *in vivo* was also investigated, using untargeted protein fRFP as a control, the probe was found accumulated stronger in human fibrocarcinoma (high integrin expression tumor) than fRFP protein at 12 h post injection (Fig. 4). In order to further investigate the biodistribution of Octa-RGD probe in inner tumors, the tumors were imaged by our lab

cyro-imager system. The tumor metabolism information has collected by imager system simultaneously (Fig. 5). The Octa-RGD probe strictly distributed in the inner tumor, while control fRFP protein not. At the same time, we also investigated the distribution of Octa-RGD probe in murine melanoma (negative integrin expression tumor), no obvious fRFP fluorescence intensity was found in the inner tumor region (data was not shown here). It further confirmed that Octa-RGD probe had chosen integrin positive cells to target, and the results were consistent with the confocal study and flow cytometry data *in vitro*.

From Figs. 4 and 5, we can conclude that the Octa-RGD probe has effective target ability to the fibrocarcinoma, while the control fRFP protein has no targeting affinity. Previous researchers considered that the tumor metabolism can affect the distribution of targeting drug,[38] we further compared the mitochondrial redox states of human fibrocarcinoma (HT1080 tumors) targeted by Octa-RGD and fRFP protein. From the results, we observed that the redox ratio and fRFP fluorescent signal of tumor samples had obvious difference between the two groups (Fig. 5). The NADH redox ratio and fRFP fluorescent signal of tumor with Octa-RGD probe distribution were much higher than the tumor with fRFP protein distribution. The fRFP had been demonstrated as a safe fluorescent indicator for *in vivo* optical imaging, and no evidence had been found that it could influence tumor metabolism.[17,18] The increased NADH redox ratio in Octa-RGD group suggests that the RGD targeting, not fRFP protein might change the tumor metabolism. It needs more experiments to confirm the relationship between RGD targeting and tumor metabolism. It had been reported that the Fp redox ratio (Fp Ratio $= 1 -$ NADH Ratio) was related to breast cancer metastatic potential. Li group observed higher Fp redox ratio in core than the rim in all aggressive tumors but not in the indolent tumors.[39] So our results may provide a new sight on RGD targeting based cancer treatment by altering tumor metabolism. Moreover, we also found that the distribution of NADH signal and fRFP was similar. To further evaluate their relationship, the correlation analysis was performed. However, no significant correlation was found (data not shown here). We hypothesized that this correlation analysis was limited by the resolution of cryo-imager, because this instrument could not distinguish whether the signal was located in tumor cells or tumor vessels. The Octa-RGD probe may remain in tumor vessels, not in inner tumor area, which may induce crosstalk in this study. It also pushes us to develop more accurate and precise instruments for detecting metabolic information in future.

In brief, we constructed a probe named Octa-RGD, which had target ability to bind integrin receptor in tumor cells surface both *in vitro* and *in vivo*. We analyzed the binding affinity of probe to a variety of tumor cells, and found that it has different affinity with tumor cells. The probe could be utilized as a useful tool for detecting integrin expression level by quantifying its fRFP fluorescence intensity in tumor cells in future. The increased NADH redox ratio of tumor with Octa-RGD probe compared to fRFP protein group also suggests that this probe might change the tumor metabolism, thus providing new insights for RGD targeting-based cancer therapeutics.

Acknowledgments

We thank the Optical Bioimaging Core Facility of WNLO-HUST for the support in data acquisition, and the Analytical and Testing Center of HUST for spectral measurements. This work was supported by the Major Research plan of the National Natural Science Foundation of China (Grant No. 91442201), the China Postdoctoral Science Foundation funded project (Grant Nos. 2015M572148, 2012M521430 and 2013T60721) and the Open Research Fund of State Key Laboratory of Bioelectronics of Southeast University. Shuang Sha and Fei Yang contributed equally to this work.

References

1. A. van der Flier, A. Sonnenberg, "Function and interactions of integrins," *Cell Tissue Res.* **305**, 285–298 (2001).
2. G. Christofori, "Changing neighbours, changing behaviour: Cell adhesion molecule-mediated signalling during tumour progression," *EMBO J.* **22**, 2318–2323 (2003).
3. R. O. Hynes, "Integrins: Bidirectional, allosteric signaling machines," *Cell* **110**, 673–687 (2002).
4. A. N. Elayadi, K. N. Samli, L. Prudkin, Y. H. Liu, A. Bian, X. J. Xie, Wistuba II, J. A. Roth, M. J. McGuire, K. C. Brown, "A peptide selected by biopanning identifies the integrin alphavbeta6 as a

prognostic biomarker for nonsmall cell lung cancer," *Cancer Res.* **67**, 5889–5895 (2007).
5. S. H. Hausner, C. K. Abbey, R. J. Bold, M. K. Gagnon, J. Marik, J. F. Marshall, C. E. Stanecki, J. L. Sutcliffe, "Targeted in vivo imaging of integrin alphavbeta6 with an improved radiotracer and its relevance in a pancreatic tumor model," *Cancer Res.* **69**, 5843–5850 (2009).
6. E. M. Nothelfer, S. Zitzmann-Kolbe, R. Garcia-Boy, S. Kramer, C. Herold-Mende, A. Altmann, M. Eisenhut, W. Mier, U. Haberkorn, "Identification and characterization of a peptide with affinity to head and neck cancer," *J. Nucl. Med.* **50**, 426–434 (2009).
7. J. R. Hsiao, Y. Chang, Y. L. Chen, S. H. Hsieh, K. F. Hsu, C. F. Wang, S. T. Tsai, Y. T. Jin, "Cyclic alphavbeta6-targeting peptide selected from biopanning with clinical potential for head and neck squamous cell carcinoma," *Head Neck* **32**, 160–172 (2010).
8. A. Eldar-Boock, K. Miller, J. Sanchis, R. Lupu, M. J. Vicent, R. Satchi-Fainaro, "Integrin-assisted drug delivery of nano-scaled polymer therapeutics bearing paclitaxel," *Biomaterials* **32**, 3862–3874 (2011).
9. K. Chen, X. Chen, "Integrin targeted delivery of chemotherapeutics," *Theranostics* **1**, 189–200 (2011).
10. J. S. Desgrosellier, D. A. Cheresh, "Integrins in cancer: Biological implications and therapeutic opportunities," *Nat. Rev. Cancer* **10**, 9–22 (2010).
11. J. Shi, Z. Jin, X. Liu, D. Fan, Y. Sun, H. Zhao, Z. Zhu, Z. Liu, B. Jia, F. Wang, "PET imaging of neovascularization with (68)Ga-3PRGD2 for assessing tumor early response to Endostar antiangiogenic therapy," *Mol. Pharm.* **11**, 3915–3922 (2014).
12. S. H. Hausner *et al.*, "Use of a peptide derived from foot-and-mouth disease," *Cancer Res.* **67** (2007).
13. R. H. Kimura, R. Teed, B. J. Hackel, M. A. Pysz, C. Z. Chuang, A. Sathirachinda, J. K. Willmann, S. S. Gambhir, "Pharmacokinetically stabilized cystine knot peptides that bind alpha-v-beta-6 integrin with single-digit nanomolar affinities for detection of pancreatic cancer," *Clin. Cancer Res.* **18**, 839–849 (2012).
14. J. S. Guthi, S. G. Yang, G. Huang, S. Li, C. Khemtong, C. W. Kessinger, M. Peyton, J. D. Minna, K. C. Brown, J. Gao, "MRI-visible micellar nanomedicine for targeted drug delivery to lung cancer cells," *Mol. Pharm.* **7**, 32–40 (2010).
15. X. Montet, K. Montet-Abou, F. Reynolds, R. Weissleder, L. Josephson, "Nanoparticle imaging of integrins on tumor cells," *Neoplasia* **8**, 214–222 (2006).
16. J. D. Keasling, A. Mendoza, P. S. Baran, "Synthesis: A constructive debate," *Nature* **492**, 188–189 (2012).
17. Shemiakina II, G. V. Ermakova, P. J. Cranfill, M. A. Baird, R. A. Evans, E. A. Souslova, D. B. Staroverov, A. Y. Gorokhovatsky, E. V. Putintseva, T. V. Gorodnicheva, T. V. Chepurnykh, L. Strukova, S. Lukyanov, A. G. Zaraisky, M. W. Davidson, D. M. Chudakov, D. Shcherbo, "A monomeric red fluorescent protein with low cytotoxicity," *Nat. Commun.* **3**, 1204 (2012).
18. D. Shcherbo, E. M. Merzlyak, T. V. Chepurnykh, A. F. Fradkov, G. V. Ermakova, E. A. Solovieva, K. A. Lukyanov, E. A. Bogdanova, A. G. Zaraisky, S. Lukyanov, D. M. Chudakov, "Bright far-red fluorescent protein for whole-body imaging," *Nat. Methods* **4**, 741–746 (2007).
19. H. Luo, J. Yang, H. Jin, C. Huang, J. Fu, F. Yang, H. Gong, S. Zeng, Q. Luo, Z. Zhang, "Tetrameric far-red fluorescent protein as a scaffold to assemble an octavalent peptide nanoprobe for enhanced tumor targeting and intracellular uptake *in vivo*," *Faseb J.* **25**, 1865–1873 (2011).
20. H. Kobayashi, R. Watanabe, P. L. Choyke, "Improving conventional enhanced permeability and retention (EPR) effects; what is the appropriate target?," *Theranostics* **4**, 81–89 (2013).
21. R. A. Cairns, I. S. Harris, T. W. Mak, "Regulation of cancer cell metabolism," *Nat. Rev. Cancer* **11**, 85–95 (2011).
22. M. R. Junttila, F. J. de Sauvage, "Influence of tumour micro-environment heterogeneity on therapeutic response," *Nature* **501**, 346–354 (2013).
23. M. Wu, A. Neilson, A. L. Swift, R. Moran, J. Tamagnine, D. Parslow, S. Armistead, K. Lemire, J. Orrell, J. Teich, S. Chomicz, D. A. Ferrick, "Multiparameter metabolic analysis reveals a close link between attenuated mitochondrial bioenergetic function and enhanced glycolysis dependency in human tumor cells," *Am. J. Physiol. Cell Physiol.* **292**, C125–136 (2007).
24. S. Walker-Samuel, R. Ramasawmy, F. Torrealdea, M. Rega, V. Rajkumar, S. P. Johnson, S. Richardson, M. Goncalves, H. G. Parkes, E. Arstad, D. L. Thomas, R. B. Pedley, M. F. Lythgoe, X. Golay, "*In vivo* imaging of glucose uptake and metabolism in tumors," *Nat. Med.* **19**, 1067–1072 (2013).
25. S. Bisdas, K. Spicer, Z. Rumboldt, "Whole-tumor perfusion CT parameters and glucose metabolism measurements in head and neck squamous cell carcinomas: A pilot study using combined positron-emission tomography/CT imaging," *AJNR Am. J. Neuroradiol.* **29**, 1376–1381 (2008).
26. B. Chance, B. Schoener, R. Oshino, F. Itshak, Y. Nakase, "Oxidation-reduction ratio studies of mitochondria in freeze-trapped samples. NADH and flavoprotein fluorescence signals," *J. Biol. Chem.* **254**, 4764–4771 (1979).

27. H. N. Xu, L. Z. Li, "Quantitative redox imaging biomarkers for studying tissue metabolic state and its heterogeneity," *J. Innov. Opt. Health. Sci.* **7**, 1430002-1-20 (2014).
28. I. E. Hassinen, "From identification of fluorescent flavoproteins to mitochondrial redox indicators in intact tissues," *J. Innov. Opt. Health. Sci.* **7** (2014).
29. T. Xiong, Z. Zhang, B. F. Liu, S. Zeng, Y. Chen, J. Chu, Q. Luo, "*In vivo* optical imaging of human adenoid cystic carcinoma cell metastasis," *Oral Oncol.* **41**, 709–715 (2005).
30. Z. Zhang, H. Li, Q. Liu, L. Zhou, M. Zhang, Q. Luo, J. Glickson, B. Chance, G. Zheng, "Metabolic imaging of tumors using intrinsic and extrinsic fluorescent markers," *Biosens. Bioelectron.* **20**, 643–650 (2004).
31. H. J. Garrigues, Y. E. Rubinchikova, C. M. Dipersio, T. M. Rose, "Integrin alphaVbeta3 Binds to the RGD motif of glycoprotein B of Kaposi's sarcoma-associated herpesvirus and functions as an RGD-dependent entry receptor," *J. Virol.* **82**, 1570–1580 (2008).
32. Z. Yang, Z. Lei, B. Li, Y. Zhou, G. M. Zhang, Z. H. Feng, B. Zhang, G. X. Shen, B. Huang, "Rapamycin inhibits lung metastasis of B16 melanoma cells through down-regulating alphav integrin expression and up-regulating apoptosis signaling," *Cancer Sci.* **101**, 494–s500 (2010).
33. A. Taherian, X. Li, Y. Liu, T. A. Haas, "Differences in integrin expression and signaling within human breast cancer cells," *BMC Cancer* **11**, 293 (2011).
34. J. Ou, W. Luan, J. Deng, R. Sa, H. Liang, "AlphaV integrin induces multicellular radioresistance in human nasopharyngeal carcinoma via activating SAPK/JNK pathway," *PLoS One* **7**, e38737 (2012).
35. A. A. Heikal, "Intracellular coenzymes as natural biomarkers for metabolic activities and mitochondrial anomalies," *Biomark. Med.* **4**, 241–263 (2010).
36. O. Tredan, C. M. Galmarini, K. Patel, I. F. Tannock, "Drug resistance and the solid tumor microenvironment," *J. Natl. Cancer Inst.* **99**, 1441–1454 (2007).
37. F. Danhier, B. Vroman, N. Lecouturier, N. Crokart, V. Pourcelle, H. Freichels, C. Jerome, J. Marchand-Brynaert, O. Feron, V. Preat, "Targeting of tumor endothelium by RGD-grafted PLGA-nanoparticles loaded with paclitaxel," *J. Control. Release* **140**, 166–173 (2009).
38. A. I. Minchinton, I. F. Tannock, "Drug penetration in solid tumours," *Nat. Rev. Cancer* **6**, 583–592 (2006).
39. H. N. Xu, S. Nioka, J. D. Glickson, B. Chance, L. Z. Li, "Quantitative mitochondrial redox imaging of breast cancer metastatic potential," *J. Biomed. Opt.* **15**, 036010 (2010).